JPE 15-2-12

http://dx.doi.org/10.6113/JPE.2015.15.2.411
ISSN(Print): 1598-2092 / ISSN(Online): 2093-4718

Estimation of ESR in the DC-Link Capacitors of AC Motor Drive Systems with a Front-End Diode Rectifier

Thanh Hai Nguyen*, Quoc Anh Le*, and Dong-Choon Lee†

*†Department of Electrical Engineering, Yeungnam University, Gyeongsan, Korea

Abstract

In this paper, a new method for the online estimation of equivalent series resistances (ESR) of the DC-link capacitors in induction machine (IM) drive systems with a front-end diode rectifier is proposed, where the ESR estimation is conducted during the regenerative operating mode of the induction machine. In the first place, a regulated AC current component is injected into the q-axis current component of the induction machine, which induces the current and voltage ripple components in the DC-link. By processing these AC signals through digital filters, the ESR can be estimated by a recursive least squares (RLS) algorithm. To acquire the AC voltage across the ESR, the DC-link voltage needs to be measured at a double sampling frequency. In addition, the ESR current is simply reconstructed from the stator currents and switching states of the inverter. Experimental results have shown that the estimation error of the ESR is about 1.2%, which is quite acceptable for condition monitoring of the capacitor.

Key words: AC machine drives, DC-link capacitors, ESR estimation, regeneration

I. Introduction

Power electronic systems play an increasingly important role in industrial applications, especially in adjustable speed machine drives, where PWM inverters have been commonly used [1]-[4]. The electrolytic capacitors in the DC link have been employed for filtering DC voltage ripples and for storing energy as a buffer [5]-[7]. One of challenging issues in the power electronic systems is the reliability of the overall system, where the power semiconductor devices and electrolytic capacitors are the most vulnerable components. According to the surveys in [8] and [9], the failure rates of the semiconductors and capacitors in power electronic converters are 21% and 30%, respectively. Hence, the electrolytic capacitor is the key component, which determines the life time of a whole system.

In order to avoid unexpected faults in a system, a reliable diagnosing technique for the DC-link capacitor in IM drive systems is essential. Many of the datasheets from capacitor manufacturers specify that the capacitor is considered to be faulty when the ESR of the capacitor increases to more than twice its initial value and the capacitance decreases to below 80% of its initial value [10]-[12]. The increase in the ESR is usually more pronounced than the decrease in the capacitance [13], [14]. Therefore, it is known that the condition monitoring of electrolytic capacitors based on variations of the ESR rather than the capacitance is more reliable.

So far, many studies have been presented for monitoring the condition of capacitors. A simple method, called as an offline method, is to disconnect the capacitor and measure its capacitance and ESR with an LCR meter [12], [15]. However, it is inconvenient to interrupt the system operation for this measurement. On the other hand, an online monitoring technique for the life-cycle condition of capacitors was proposed [13], where the ESR of the capacitor is estimated from the capacitor losses which are calculated from the capacitor voltage and current. This method requires an additional circuit for acquiring the voltage and current. Another technique that applies to adjustable-speed machine drives has been presented in [16], where the condition of the DC-link electrolytic capacitors is monitored based on the estimated values of the ESR and capacitance, which are calculated from the inverter side when the motor stops. In this method, complicated signal processing for the measured

Manuscript received Sep. 12, 2014; accepted Nov. 16, 2014
Recommended for publication by Associate Editor Kwang-Woon Lee.
†Corresponding Author: dclee@yu.ac.kr
Tel: +82-53-810-2582, Fax: +82-53-810-4767, Yeungnam University
*Department of Electrical Engineering, Yeungnam University, Korea

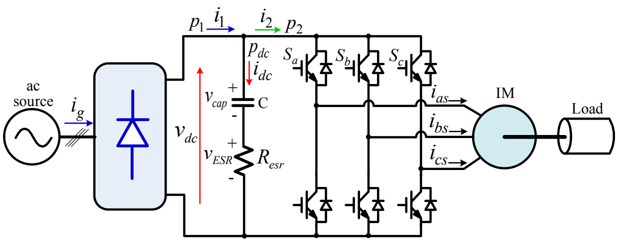

Fig. 1. Induction machine drive system with a front-end diode rectifier.

voltage and current is needed. On the other hand, an ESR estimation method for the DC-link capacitor of an AC/DC PWM converter was introduced by utilizing current injection [14], where the ESR is calculated from the instantaneous values of the voltage and current in the ESR at the mid-point instant of the sampling period under the no load condition. Recently, an estimation method of the capacitance of DC-link capacitors has been proposed for AC machine drive systems with a front-end diode rectifier, where it is possible to achieve the regenerative operating mode [17], [18].

In this paper, a new method for the online estimation of ESR in the DC-link capacitors of AC machine drives is proposed, by which the deterioration condition of a DC-link capacitor can be diagnosed. An IM drive fed by a VSI (voltage-source inverter) through a coupling of the DC-link capacitor with a front-end diode rectifier is shown in Fig. 1. The DC-link capacitor is usually modeled as an ESR in series with a capacitance. The ESR is estimated from the AC components of the voltage and the current ripples in the DC link, which are produced by the AC current injected into the q-axis current component in the machine side. For the controller, PR (proportional resonant) controllers are used to regulate the AC component of the q-axis current, whereas PI (proportional integral) controllers are used for the DC component of the q-axis current generated from the speed controller and the d-axis current. The capacitor current can be calculated from only the stator currents since the diode rectifier is blocked while the induction motor is in the regenerative operating mode. An experimental test on a 3-kW IM drive is carried out to verify the validity of the proposed method. The experimental results show that the proposed technique gives a reliable result with an ESR estimation error of 1.2%.

II. Relationship of the Voltages in the DC Link for the PWM Switching Period

The relationship of the voltages and current in the DC link of a voltage source inverter for the PWM switching interval is briefly described below. It is similar to the concept in the AC/DC PWM converter in [14].

With the switching states of the VSI, the instantaneous DC-link current is reproduced from the motor phase currents which also defines the relationship between the DC-link voltage and the capacitor voltage, which is shown in Fig. 2.

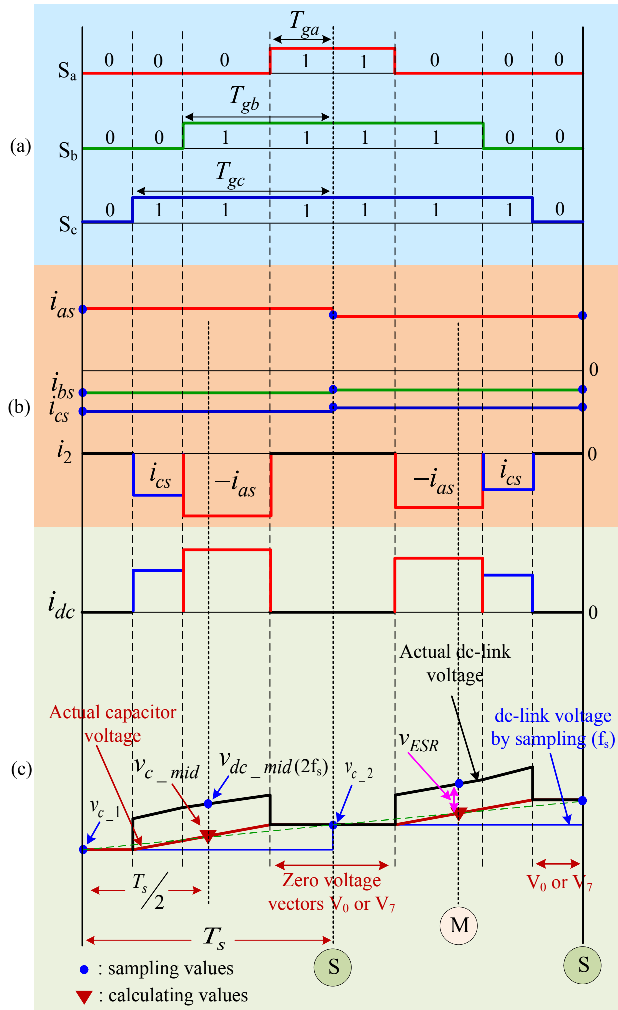

Fig. 2. Details in the DC link. (a) Switching states. (b) Stator currents and instantaneous DC-link current. (c) Relationship of voltages and current in the DC link.

The switching states and gating times for the upper switches of each inverter leg are denoted as S_a, S_b, and S_c, and T_{ga}, T_{gb}, and T_{gc}, as shown in Fig. 2, and T_s is the sampling time. The instantaneous DC-link current can be calculated from the stator phase currents and the switching states of the inverter as [14]:

$$i_2 = S_a i_{as} + S_b i_{bs} + S_c i_{cs} \tag{1}$$

where i_2 is the instantaneous DC-link current, and i_{as}, i_{bs}, and i_{cs} are the stator currents. It is illustrated in Fig. 2(a) - (b) and (1) that the instantaneous DC-link current is zero during the interval of the zero voltage vectors, where all of the upper or lower switches turn on or off simultaneously. During the regenerative mode of the machine, the capacitor current is identical to the negative of the DC-link current due to the blocking sate of the diode rectifier ($i_1 = 0$), which is shown in Fig. 2(b) -(c) and expressed as:

$$i_{dc} = -i_2 \tag{2}$$

where i_{dc} is the capacitor current.

As shown in Fig. 1, the DC-link voltage, v_{dc}, is a summation of the capacitance voltage, v_{cap}, and the ESR voltage, v_{ESR}, which is expressed as:

$$v_{dc} = v_{cap} + v_{ESR} = v_{cap} + R_{esr} \cdot i_{dc} \tag{3}$$

where R_{esr} is the ESR of the DC-link capacitor.

It is known that the DC-link voltage in the VSI is usually measured at the interval of the zero voltage vectors for every sampling period. In this period, from (1) and (2), (3) can be rewritten as:

$$v_{dc} = v_{cap}. \tag{4}$$

It can also be seen in Fig. 2 that for the interval of the active voltage vectors, there is a current flowing through the DC capacitor, which results in a voltage drop across the ESR, as shown in the bottom waveform in Fig. 2.

III. Control of IM Drives for ESR Estimation of DC-Link Capacitors

As previously mentioned, the ESR of the DC-link capacitors in IM drives is estimated during the regenerative operation. Here, the regenerative operating principle and the control of the induction motor are shortly described [17].

The power balance for an IM drive system is expressed as [19]:

$$p_1 = p_2 + p_{dc} = p_2 + Cv_{cap}\frac{dv_{cap}}{dt} + R_{esr} i_{dc}^2 \tag{5}$$

$$p_2 = J\omega_m \frac{d\omega_m}{dt} + P_{load} + P_{loss} \tag{6}$$

where p_1 and p_2 are the DC-link input and output powers, p_{dc} is the DC-link power, C is the capacitance of the DC-link capacitor, J is the inertia of the drive system, ω_m is the machine speed, P_{load} is the load power applied to the machine, and P_{loss} is the loss in both the VSI and machine.

Fig. 3 shows a control block diagram of the induction machine [20]. The q-axis current reference is produced from the outer speed control loop. Then, the inner dq-axis current loops are employed to control the rotor flux and the machine torque, where the d-axis current is controlled at a constant value of 5 A. To acquire AC signals from the voltage and current of the DC link, an AC current component, $i^*_{qse\_inj}(t)$, is injected into the q-axis stator current during the estimation process, of which the waveform is sinusoidal beginning at a zero in order to avoid a large transient for the current

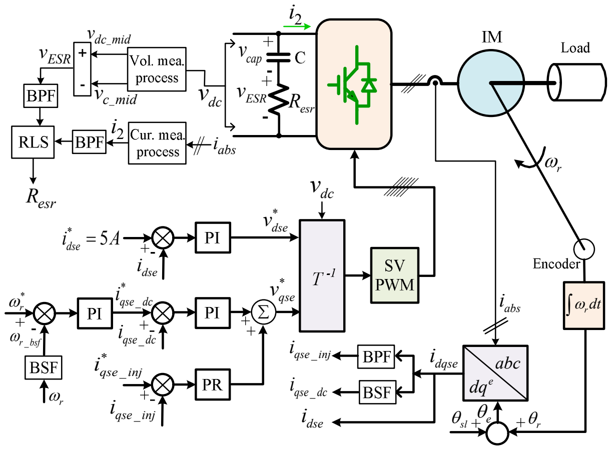

Fig. 3. Control block diagram of IM for ESR estimation.

control, which is expressed as:

$$i^*_{qse\_inj}(t) = I_{inj}\sin(2\pi f_{inj} t) \tag{7}$$

where I_{inj} and f_{inj} are the magnitude and frequency of the injected current, respectively. By this injection, the motor torque ripple and the speed pulsation are induced. They are limited to an allowable range with an appropriate selection of the magnitude of the injected current. It is noted that the estimation duration is very short, which has a slight effect on the operation of the motor. The selection criteria for the frequency and magnitude of the AC injected current has been described in detail in [17]. According to this criteria, the values 30 Hz and 3 A are used in this work.

As shown in Fig. 3, PR regulators are used to control the injected AC component of the q-axis current, whereas PI controllers are employed to regulate the DC components of the q-axis currents and the d-axis current. For the feedback control, a band-pass filter (BPF) and band-stop filters (BSF) with a cut-off frequency of 30 Hz are employed to extract the AC and DC components of the q-axis current as well as the machine speed.

IV. Proposed Scheme for ESR Estimation

The ESR of the DC-link capacitor is calculated from the voltage across the ESR and the current flowing through the ESR, which is expressed as:

$$R_{esr} = \frac{v_{ESR}}{i_{dc}}. \tag{8}$$

A. Calculation of Voltage across the ESR

A process to calculate the ESR voltage in the DC-link capacitor of the AC/DC PWM converter can be applied to the VSI of AC machine drive systems, which is briefly explained as follows.

As previously mentioned, the DC voltage is usually sensed for the interval of the zero voltage vector at point S, as shown in Fig. 2, where no current flows through the ESR, resulting in a zero voltage drop across the ESR. However, it is shown in Fig. 2(c) that there is a difference between the actual DC-link and capacitor voltages for the interval of the active voltage vectors, which is the ESR voltage. Therefore, to acquire the ESR voltage, the DC voltage needs to be sampled for the interval of the active voltage vectors [14]. In this study, the capacitor voltage is measured at the instant of the zero voltage vectors, whereas the midpoint values of the DC-link voltage, consisting of the capacitor voltage and the ESR voltage, can be sensed by doubling the sampling frequency, $v_{dc\_mid(2f_s)}$, at point M, as shown in Fig. 2.

The midpoint value of the capacitor voltage, v_{c_mid}, is calculated as the average value of two consecutive DC-link voltages, which is depicted in Fig. 2(c) and expressed as [14]:

$$v_{c\_mid} = \frac{v_{c\_1} + v_{c\_2}}{2} \tag{9}$$

where v_{c_1} and v_{c_2} are the DC-link voltages sensed for the interval of the zero voltage vectors.

Then, the voltage drop across the ESR can be calculated as:

$$v_{ESR} = v_{dc\_mid(2f_s)} - v_{c\_mid}. \tag{10}$$

B. Reconstruction of Capacitor Current

The instantaneous DC-link current in (1) is a pulse-wise waveform, where the switching functions (S_a, S_b, and S_c) are required to reconstruct the DC-link current. For easy implementation in practical applications, the DC-link current is reconstructed from the phase currents and the gating times of the VSI instead of the switching functions. For ESR calculation, the mean value of the capacitor current, $i_{2,cal}$, during the active voltage vectors is required, which is expressed as [21]:

$$i_{2,cal} = \frac{T_{ga} i_{sa} + T_{gb} i_{sb} + T_{gc} i_{sc}}{T_{\max} - T_{\min}} \tag{11}$$

where $T_{\max}$ and $T_{\min}$ are the maximum and minimum gating times of (T_{ga}, T_{gb}, and T_{gc}), respectively.

Then, the average value of the capacitor current, $i_{dc,cal}$, in a sampling period is obtained as:

$$i_{dc,cal} = -i_{2,cal}. \tag{12}$$

C. Estimation of ESR in the DC-Link Capacitor

Eq. (8) can be rewritten with (11) and (12) as:

$$v_{ESR} = R_{esr} \cdot i_{dc,cal}. \tag{13}$$

In this study, the mean value of the reconstructed capacitor current in a sampling period is used for the estimation process, instead of the mid-point values of the capacitor current which require complicated signal processing [14].

Then, by applying band-pass filters with a cut-off frequency of 30 Hz on both sides of (13), only the AC components of the ESR voltage and current only processed, resulting in:

$$BPF[v_{ESR}] = R_{esr} \cdot BPF[i_{dc,cal}] \tag{14}$$

where $BPF[\cdot]$ represents the band-pass filtered signal.

Since the ESR estimated from the voltage and current usually contains a ripple, an RLS algorithm is applied for a reliable estimation. It is well known that the RLS algorithm is used to minimize the least square cost function in each sampling period whenever a data is updated. An error cost function for (14) is defined as [21], [22]:

$$e^2(k) = \left[BPF[v_{ESR}(k)] - \hat{R}_{esr}(k) \cdot BPF[i_{dc,cal}(k)] \right]^2 \tag{15}$$

where $\hat{R}_{esr}$ is the estimated value of the ESR.

From (15), the gradient of the error with respect to $\hat{R}_{esr}(k)$ is given as:

$$\frac{\partial e^2(k)}{\partial \hat{R}_{esr}(k)} = -2BPF[i_{dc,cal}(k)] \times \left[BPF[v_{ESR}(k)] - \hat{R}_{esr}(k) \cdot BPF[i_{dc,cal}(k)] \right]. \tag{16}$$

To minimize the error cost function, $e^2(k)$, $\hat{R}_{esr}$ should be updated as illustrated in (16). Therefore, the updated ESR value by the RLS algorithm is given as:

$$\hat{R}_{esr}(k+1) = \hat{R}_{esr}(k) + \gamma(k) BPF[i_{dc,cal}(k)] \times \left[BPF[v_{ESR}(k)] - \hat{R}_{esr}(k) \cdot BPF[i_{dc,cal}(k)] \right] \tag{17}$$

where $\gamma(k)$ is an adjustable gain that was selected, by the trial and error method, as a constant of 1.2×10^{-6}. The procedure to estimate the ESR is illustrated in Fig. 3 (in the top left side).

V. Experimental Results

To confirm the effectiveness of the proposed scheme, an experimental test is carried out on a prototype of an IM drive system in the laboratory, which is illustrated in Fig. 4. The hardware setup consists of a 3-kW SCIM (squirrel-cage induction motor) coupled with a PMSG (permanent-magnet synchronous generator) to apply a load. A front-end diode rectifier supplied by a 3-phase AC source of 215V/60Hz is used to provide the input voltage for the VSI. A digital controller based on a DSP TMS320VC33 chip was used to control the IGBT inverter, where the switching frequency is 3.33 kHz. The sampling periods of the current and speed control loops are 150 μs and 1.5 ms, respectively. The parameters of the IM drive are listed in Table I. Four sound capacitors were used in the DC link, where the capacitors are

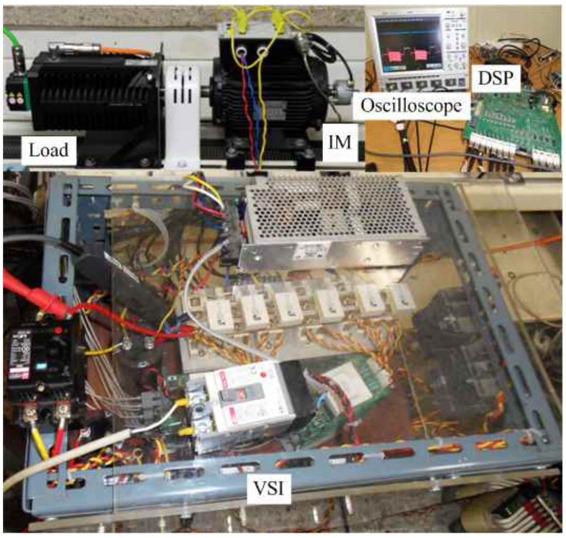

Fig. 4. Experimental setup.

TABLE I

PARAMETERS OF INDUCTION MACHINE

Rated power	3 kW
Stator voltage/frequency	220 V/60 Hz
Stator resistance	0.533 Ω
Rotor resistance	0.93 Ω
Stator/rotor inductance	3 mH
Magnetizing inductance	76 mH
Number of poles	4
Total inertia of drive system	0.00931 kg.m^2
Friction coefficient of drive system	0.00435 Nm/rad/s

TABLE II

PARAMETERS OF DC-LINK CAPACITOR

DC-link capacitor	C (measured)	R_{esr} (measured)
Connection 1	727 μF	0.127 Ω
Connection 2	1,590 μF	0.0535 Ω

connected in series and parallel. Connection 1 consists of three capacitors connected in series, whereas connection 2 is composed of two capacitors connected in parallel, which are in series with the other two capacitors. The parameters of the effective DC-link capacitor and ESR for the two connections are listed in Table II.

The performance of the IM control is shown in Fig. 5 for the ESR estimation process with connection 1 of the DC-link capacitor, in which the machine speed is reduced from 1,500 rpm with a deceleration rate of 204 rad/s^2 from 0.6 s for the regenerative operation as shown in Fig. 5(a). Fig. 5(b) shows the d-axis stator currents, which are regulated at the rated value of 5 A for excitation. The q-axis stator current consists of the DC and AC injected components as shown in Fig. 5(c) and (d), respectively. It can be seen in Fig. 5(c) that the DC component of the q-axis stator current is negative, which implies that the power from the machine flows back to the DC-link capacitor due to the deceleration operation. Under the no load condition, the q-axis stator current also exists as

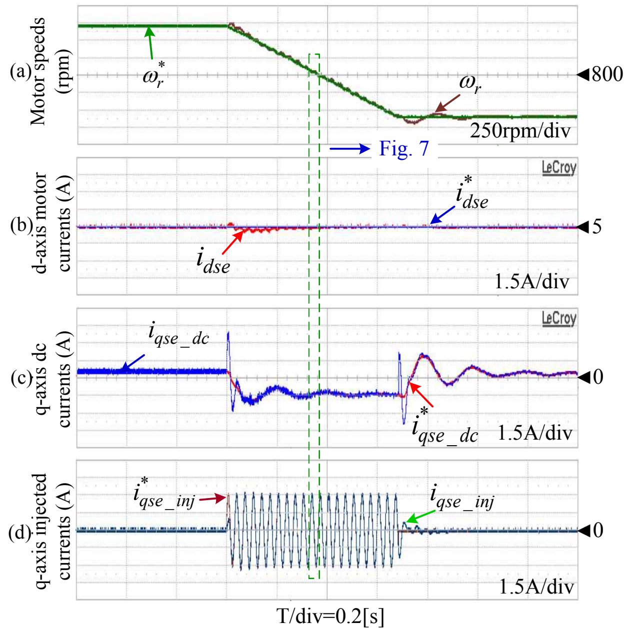

Fig. 5. Control of IM for the estimation process. (a) Machine speeds. (b) d-axis components of stator current. (c) DC components of q-axis stator current. (d) AC components of q-axis stator current.

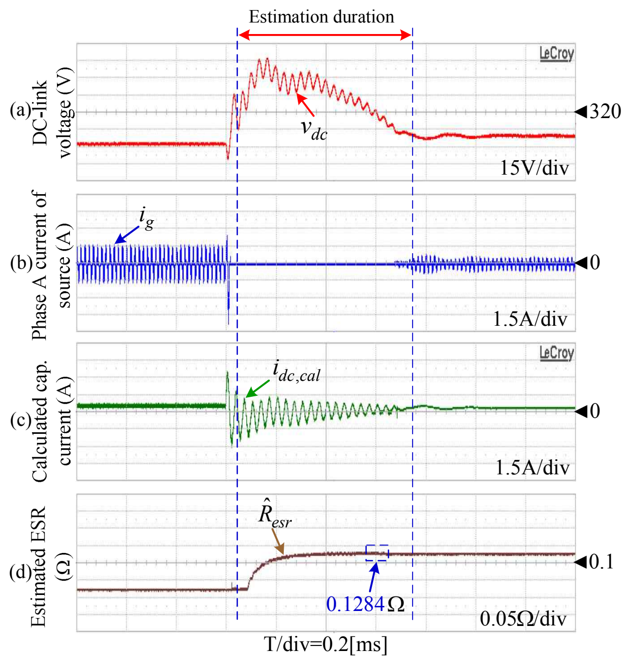

Fig. 6. Behavior of DC-link and AC sides during deceleration mode. (a) DC-link voltage. (b) Source phase current. (c) Reconstructed capacitor current. (d) Estimated ESR value.

shown in Fig. 5(c). The AC injected component of the q-axis stator current is well regulated by the PR controller as shown in Fig. 5(d).

The response of the DC-link and input AC sides during the deceleration of the machine is shown in Fig. 6. Fig. 6(a) shows the DC-link voltage. It can be seen that during the

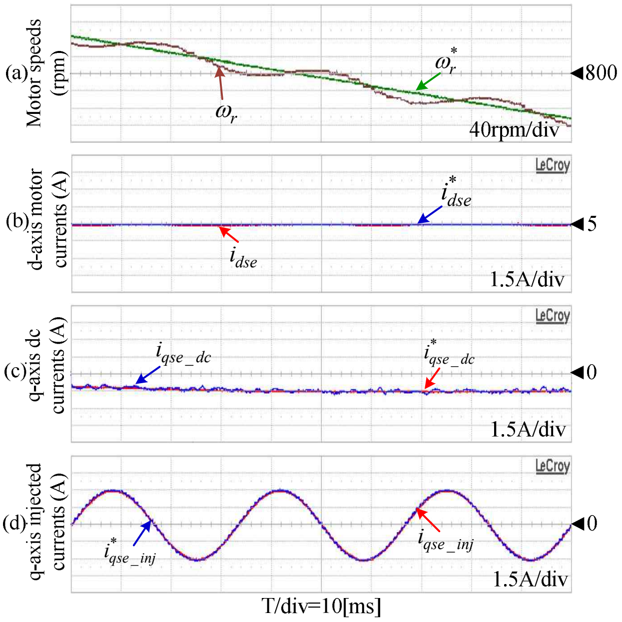

Fig. 7. Control of IM during the estimation process (magnified waveforms from Fig. 5). (a) Speeds of machine. (b) d-axis components of stator current. (c) DC components of q-axis stator current. (d) AC components of q-axis stator current.

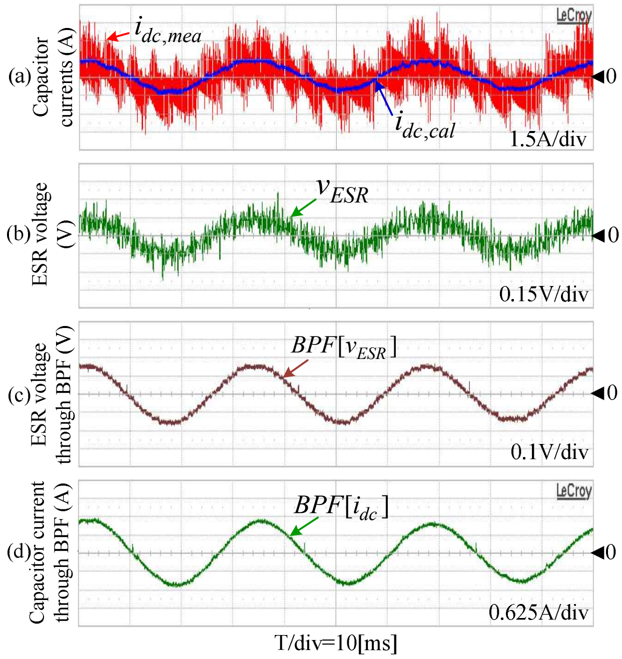

Fig. 8. Signal processing in the DC link. (a) Capacitor currents. (b) ESR voltage. (c) Band-pass filtered ESR voltage. (d) Band-pass filtered capacitor current.

regenerative operation, the DC-link voltage is increased higher than that of in the motoring operation. With this DC-link voltage, the diode rectifier is blocked, resulting in no current flowing from the AC source to the DC-link side in this interval as shown in Fig. 6(b). Fig. 6(c) shows the reconstructed capacitor current. Through the signal processing of the DC-link voltage and current, the AC components of the ESR voltage and current are acquired. Then, the ESR of the DC-link capacitor is calculated according to (16) as shown in Fig. 6(d), in which the estimation error is about 1.2%. Then, the deterioration condition of the capacitor can be monitored with a consideration of the effect of temperature on the ESR, where the estimated ESR value is compared with the referred initial value with regard to the operating temperature. Even though its effect has not been investigated in this study, it can be simply implemented, and has been described in detail in [14].

Fig. 7 shows magnified waveforms from Fig. 5, where the sensed speed and its reference are shown in Fig. 7(a). It can be seen from Fig. 7(a) that the actual machine speed fluctuates a little, which is only about 2.5% compared with the operating speed. The speed fluctuation depends on the frequency of the injected current and the machine inertia. Due to this ripple component of the machine speed, the BSF needs to acquire the feedback signal for the speed controller as shown in Fig. 3. By virtue of the BSF, the speed controller works well. The d-axis stator currents are shown in Fig. 7(b). Fig. 7(c) and (d) show the DC and AC components of the q-axis stator current, respectively, which are kept close to their references.

Fig. 8 shows the signals of the processed DC-link voltage and current. The DC-link currents are shown in Fig. 8(a), where the average value of the reconstructed current, $i_{dc,cal}$, is almost equal to that of the quantity measured directly by the probe, $i_{dc,mea}$. Fig. 8(b) shows the ESR voltage, which is acquired from the sensed and calculated values of the DC-link voltage as shown in (10). It can also be seen that the ESR voltage contains a30-Hz ripple component with the same frequency as that of the injected current. The ESR voltage and capacitor current are filtered out by the BPF with a 30-Hz cutoff frequency, as shown in Fig. 8(c) and (d), respectively.

Fig. 9 shows the estimations of the ESR values in the extreme case of an abrupt variation under the conditions of Table II. First, connection 2 of the DC-link capacitor is applied, and then it is changed to connection 1 by disconnecting the parallel-connected capacitor with a circuit breaker at 6.8 s. Fig. 9(a) shows the machine speed, where the machine is operated under the regenerating mode twice for 2 s ~ 2.7 s and 6.75 s ~ 7.45 s. During this operation, the current controllers of the dq-axis stator currents still work well as shown in Fig. 9(b) and (c), respectively. Fig. 9(d) shows the DC-link voltage, which is greatly increased during the deceleration operations of the machine. It can be seen in Fig. 9(d) that the DC-link voltage during the second regenerative operation is higher than that in the first one due to a reduction of the DC-link capacitance in the second operation. Fig. 9(e) shows the phase-A current of the source,

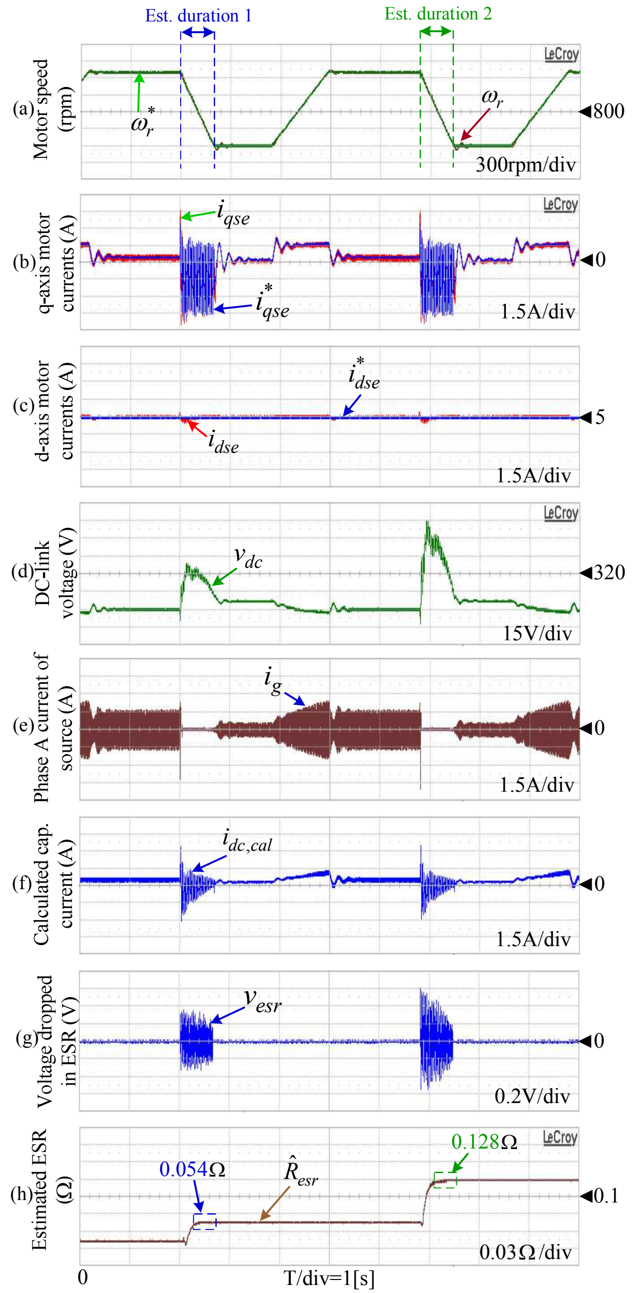

Fig. 9. Estimation in an abrupt variation of ESR of DC-link capacitor. (a) Motor speeds. (b) q-axis stator currents. (c) d-axis stator currents. (d) DC-link voltage. (e) Phase-A current of source. (f) DC-link current. (g) ESR voltage. (h) Estimated ESR.

where no current flows into the DC-link side from the source during deceleration. The capacitor current is shown in Fig. 9(f). Fig. 9(g) shows the voltage drop across the ESR, where the ESR voltage during the second deceleration is higher than that in the first deceleration due to an increase in the ESR value of the DC-link capacitor. The ESR value is calculated as shown in Fig. 9(h). It can be seen that the estimation errors for the two cases are less than 1.2%. In addition, it can be seen in Fig. 9(h) that the estimation is fast enough for the variation of the ESR of the capacitor.

VI. Conclusions

In this paper, a novel online estimation scheme for the ESR of the DC-link capacitors in AC machine drive systems has been proposed. The regenerative operation of the machine is utilized, which increases the DC-link voltage, causing a blocking of the diode rectifier. Then, the DC-link current can be directly calculated by the stator currents and the switching times of the VSI. Injecting the AC regulated current component into the q-axis stator current induces AC current and voltage components in the DC link as well as in the ESR of the capacitor, where the RLS algorithm is applied to achieve a reliable estimation of the ESR. In this proposed method, no additional hardware is required. It can be implemented simply in practical machine drive systems. However, the proposed scheme has a limitation in that it can only estimate the total capacitance of the DC-link capacitors, but not individually for a capacitor bank with multiple units. Experimental results obtained witha3-kW IM drive system in the laboratory have shown that the estimation error of the proposed method is less than 1.2%, by which the fault diagnosis of the DC-link capacitor is performed.

Acknowledgment

This research was supported by the Yeungnam University Research Grants in 2012.

References

[1] S.-H. Hwang and J.-M. Kim, “Dead time compensation method for voltage-fed PWM inverter,” *IEEE Trans. Energy Convers.*, Vol. 25, No. 1, pp. 1-10, Mar. 2010.

[2] T. H. Nguyen, T. L. Van, D. C. Lee, J.-H. Park, and J.-H Hwang, “Control mode switching of induction machine drives between vector control and V/f control in overmodulation range,” *Journal of Power Electronics*, Vol. 11, No. 6, pp. 846-855, Nov. 2011.

[3] J. Zhang, J. Zhao, D. Zhou, and C. Huang, “High-performance fault diagnosis in PWM voltage-source inverters for vector-controlled induction motor drives,” *IEEE Trans. Power Electron.*, Vol. 29, No. 11, pp. 6087-6099, Nov. 2014.

[4] X. Li and S. Li, “Speed control for a PMSM servo system using model reference adaptive control and an extended state observer,” *Journal of Power Electronics,* Vol. 14, No. 3, pp. 549-563, May 2014.

[5] M. A. Vogelsberger, T. Wiesinger, and H. Ertl, “Life-cycle monitoring and voltage managing unit for DC-link electrolytic capacitors in PWM converters,” *IEEE Trans. Power Electron.,* Vol. 26, No. 2, pp. 493-503, Feb. 2011.

[6] K. Abdennadher, P. Venet, G. Rojat, J. M. Retif, and C. Rosset, “A real-time predictive-maintenance system of aluminum electrolytic capacitors used in uninterrupted power supplies,” *IEEE Trans. Ind. Appl.,* Vol. 46, No. 4, pp. 1644-1652, Jul./Aug. 2010.

[7] A. G. Abo-Khalil and D.-C. Lee, “DC-link capacitance estimation in AC/DC/AC PWM converters using voltage injection,” *IEEE Trans. Ind. Appl.,* Vol. 44, No. 5, pp. 1631-1637, Sep./Oct. 2008.

[8] S. Yang, D. Xiang, A. Bryant, P. Mawby, L. Ran, and P. Tavner, "Condition monitoring for device reliability in power electronic converters: a review," *IEEE Trans. Power Electron.*, Vol. 25, No. 11, pp. 2734-2752,Nov. 2010.
[9] M. Boetthias and F. W. Fuchs, "Power electronic converters in wind energy systems - considerations of reliability and strategies for increasing availability," in *Proc. of EPE*, pp. 1-10, 2011.
[10] http://www.tawelectronics.com/xicon/XICON_LS.pdf.
[11] http://www.chemi-con.com/images/stories/al-kmqlg-e-120701.pdf
[12] A. M. R. Amaral and A. J. M. Cardoso, "A simple offline technique for evaluating the condition of aluminum-electrolytic capacitors," *IEEE Trans. Ind. Electron.,* Vol. 56, No. 8, pp. 3230-3237, Aug. 2009.
[13] M. A. Vogelsberger, T. Wiesinger, and H. Ertl, "Life-cycle monitoring and voltage-managing unit for DC-link electrolytic capacitors in PWM converters," *IEEE Trans. Power Electron.*, Vol. 26, No. 2, pp. 493–503, Feb. 2011.
[14] X. S. Pu, T. H. Nguyen, D.-C. Lee, K.-B. Lee, and J.-M. Kim, "Fault diagnosis of DC-link capacitors in three-phase AC/DC PWM converters by online estimation of equivalent series resistance," *IEEE Trans. Ind. Electron.,* Vol. 60, No. 9, pp. 4118-4127, Sep. 2013.
[15] K. Harada, A. Katsuki, and M. Fujiwara, "Use of ESR for deterioration diagnosis of electrolytic capacitor," *IEEE Trans. Power Electron.*, Vol. 8, No. 4, pp. 355–361, Oct. 1993.
[16] K. W. Lee, M. Kim, J. Yoon, S. B. Lee, and J. Y. Yoo, "Condition monitoring of DC-link electrolytic capacitors in adjustable-speed drives," *IEEE Trans. Ind. App.,* Vol. 40, No. 5, pp. 1606-1613, Sep./Oct. 2008.
[17] T. H. Nguyen and D.-C. Lee, "Deterioration monitoring of DC-link capacitors in ac machine drives by current injection," *IEEE Trans. Power Electron.*, Vol. 30, No. 3, pp. 1126-1130, Mar. 2015.
[18] J.-J. Moon, W.-S. Im, and J.-M. Kim, "Capacitance estimation of DC-link capacitor in brushless DC motor drive systems," in *Proc. of IEEE ECCE Asia 2013*, Australia, pp. 525-529, Jun. 2013.
[19] S.-K. Sul, *Control of Electrical Machine Drive Systems*, Wiley & Sons, 2011
[20] M. H. N. Talib, Z. Ibrahim, N. A. Rahim, and A. S. A. Hasim, "Implementation of space vector two-arm modulation for independent motor control drive fed by a five-leg inverter," *Journal of Power Electronics,* Vol. 14, No. 1, pp. 115-124, Jan. 2014.
[21] D.-C. Lee, K.-J. Lee, J.-K. Seok, and J.-W. Choi, "Online capacitance estimation of DC-link electrolytic capacitors for three-phase AC/DC/AC PWM converters using recursive least squares method," *IEE Proc. Electric Power Appl.*, Vol. 152, No. 6, pp. 1503-1508, Nov. 2005.
[22] I. Sadinezhad and V. G. Agelidis, "Frequency adaptive least-squares- Kalman technique for real-time voltage envelope and flicker estimation," *IEEE Trans. Ind. Electron.*, Vol. 59, No. 8, pp. 3330-3041, Aug. 2012.

Thanh Hai Nguyen was born in Dong Thap, Vietnam. He received his B.S. degree in Electrical Engineering from the Ho Chi Minh City University of Technology, Ho Chi Minh City, Vietnam, in 2003, and his M.S. and Ph.D. degrees in Electrical Engineering from Yeungnam University, Gyeongbuk, Korea, in 2010 and 2013, respectively. He is presently working as a Research Professor at Yeungnam University. From May 2003 to February 2008, he was an Assistant Lecturer in the College of Technology, Can Tho University, Can Tho, Vietnam. His current research interests include power converters, machine drives, HVDC transmission systems, and wind power generation.

Quoc Anh Le was born in Can Tho, Vietnam, in 1988. He received his B.S. degree in Electrical Engineering from Can Tho University, Can Tho, Vietnam, in 2010, and his M.S. degree from the Ho Chi Minh City University of Technology, Ho Chi Minh City, Vietnam, in 2013. He is presently working toward his Ph.D. degree in the Department of Electrical Engineering, Yeungnam University, Gyeongbuk, Korea. In 2011, he was an Assistant Lecturer in the College of Technology, Can Tho University. His current research interests include high power converters and multi-level converters.

Dong-Choon Lee received his B.S., M.S., and Ph.D. degrees in Electrical Engineering from Seoul National University, Seoul, Korea, in 1985, 1987, and 1993, respectively. He was a Research Engineer with Daewoo Heavy Industry, Korea, from 1987 to 1988. Since 1994, he has been a faculty member in the Department of Electrical Engineering, Yeungnam University, Gyeongbuk, Korea. As a Visiting Scholar, he joined the Power Quality Laboratory, Texas A&M University, College Station, TX, USA, in 1998; the Electrical Drive Center, University of Nottingham, Nottingham, UK, in 2001; the Wisconsin Electric Machines and Power Electronic Consortium, University of Wisconsin, Madison, WI, USA, in 2004; and the FREEDM Systems Center, North Carolina State University, Raleigh, NC, USA, from September 2011 to August 2012. His current research interests include ac machine drives, the control of power converters, wind power generation, and power quality. Professor Lee is currently the Editor-in-Chief for the *Journal of Power Electronics* of the Korean Institute of Power Electronics.